Radiation as a physical probe

Cormac Purcell

The University of Sydney

June 26, 2012

1 Introduction

Our sole window on the environment of molecular clouds is provided by radiation from astrophysical processes. Gas in star-forming environments may both emit and absorb spectral line and continuum radiation, whose properties can be used to derive physical and chemical conditions. This document begins with a description of how radiation and molecules interact to form rotational spectra in the millimetre regime. The statistical emission and absorption properties of the gas are then used to explain how radiation is transmitted through the interstellar medium, allowing the derivation of physical parameters from observations. Lastly, the spectrum of the versatile molecular thermometer NH_3 is described and the analysis methodology presented as a case study. The following discussion borrows heavily from Townes & Schawlow (1955), Rohlfs & Wilson (2004) and Goldsmith & Langer (1999), whose formalisms have been adopted here. Unless specifically stated all equations and quantities are presented in the SI (MKS) unit system.

2 Rotational spectral lines

In the gas phase, ensembles of molecules are in constant motion related to bulk motions, turbulence and their thermal kinetic energy. In addition, individual molecules have internal energy, a portion of which is stored as rotational energy. For an isolated molecule, its angular momentum is quantised in multiples of $\hbar = h/2\pi$. The rotation of any molecule may be resolved into components about three perpendicular axes through the centre of mass. Classically, rotation is described in terms of the moment of inertia I about a particular axis. This is defined as

$$I = \sum m_i r_i^2, \tag{1}$$

where r_i is the perpendicular distance of the ith atom from the axis of rotation, and m_i is its mass. A rotating body with three degrees of freedom has a total kinetic energy

$$E = \frac{1}{2} \left[I_a \omega_a^2 + I_b \omega_b^2 + I_c \omega_c^2 \right], \tag{2}$$

where ω_a is the angular velocity in radians/sec about an axis 'a'. Equation 2 may be written in terms of the classical angular momentum, $P_a = I_a \omega_a$:

$$E = \frac{P_a^2}{2I_a} + \frac{P_b^2}{2I_b} + \frac{P_c^2}{2I_c}, \tag{3}$$

with the magnitude of the total angular momentum given by $P^2 = P_a^2 + P_b^2 + P_c^2$.

Molecular rotors fall into four groups, according to the relative values of their three moments of inertia:

Spherical Rotors:	$I_a = I_b = I_c$,	e.g., CH_4, SiH_4.
Linear Rotors:	$I_a = 0, I_b = I_c$,	e.g., CO, HCO+, HCN, HNC, N_2H^+
Symmetric Rotors:	$I_a = I_b \neq I_c$,	e.g., NH_3, CH_3CN, CH_3Cl.
Asymmetric Rotors:	$I_a \neq I_b \neq I_c$,	e.g., H_2O, CH_3OH.

To emit or absorb radiation efficiently the molecule must have a permanent dipole moment, μ[1]. Usually the dipole is an electric moment due to the asymmetric distribution of positive and negative charges on a molecule. The electronic charge on spherical and homo-nuclear linear molecules is evenly distributed and these molecules do not exhibit rotational dipole transitions. Instead much weaker quadrupole lines are observed in the infrared, due to simple collisional excitation. The quadrupole arises from the interaction of external electromagnetic fields with the slightly asymmetric charge distribution in the nucleus.

In the following sections we will summarise the theory necessary to derive physical properties from the spectra of symmetric and linear rotors.

2.1 Rotational energy levels

Symmetric rotors have one unique axis $(I_c \equiv I_\parallel)$, called the principal axis, and two identical axes $(I_a = I_b \equiv I_\perp)$ perpendicular to it. The energy of a symmetric rotor may be found from Equation 3

$$E = \frac{P^2}{2I_\perp} - \frac{P_c^2}{2I_\perp} + \frac{P_c^2}{2I_\parallel} = \frac{P^2}{2I_\perp} + \left(\frac{1}{2I_\parallel} - \frac{1}{2I_\perp} \right) P_c^2, \tag{4}$$

and the quantised expression for rotational energy levels can be obtained from the Correspondence Principle by substituting the angular momentum operator, $J^2 \rightarrow J(J+1)\hbar^2$, for P in Equation 4. We know that the projection of the total angular momentum onto the principal axis is restricted to values of $K\hbar$, with $K = 0, \pm1, \pm2, \ldots \pm J$, so J_c^2 is also replaced by $K^2\hbar^2$. The energy levels are then given by

$$E_{J,K} = hBJ(J+1) + h(A-B)K^2 \tag{5}$$

with

$$A = \frac{\hbar}{4\pi I_\parallel} \quad \text{and} \quad B = \frac{\hbar}{4\pi I_\perp} \tag{6}$$

defined as the rotational constants of the molecule. The units of the rotational constants are Hz.

Linear rotors can be considered a special case of symmetric top, which only rotate perpendicular to the principal axis, therefore the projection of the total angular momentum onto this axis is zero, i.e., K=0. In this case Equation 5 reduces to

$$E_J = hBJ(J+1) \tag{7}$$

for linear molecules and $A \equiv 0$.

2.2 Form of the rotational spectrum

Even simple molecules can have complicated spectra. The wavelength of a spectral line and its intensity are related to the intrinsic properties of the molecule and transition, but the physical and chemical conditions of the gas determine the final intensity and shape of the spectral lines. Quantum selection rules and centripetal distortion determine the frequencies of allowed spectral lines and the intensity is governed by the intrinsic permanent dipole moment, the degeneracy of the energy level, and the temperature, density and abundance of the gas. The following sections present the basic molecular theory from which we can derive physical properties from observed spectral lines.

---

[1]Molecules without a permanent dipole moment can couple to external radiation fields via higher moments, e.g., H_2 and N_2 exhibit quadrupole transitions, however these lines are usually weak.
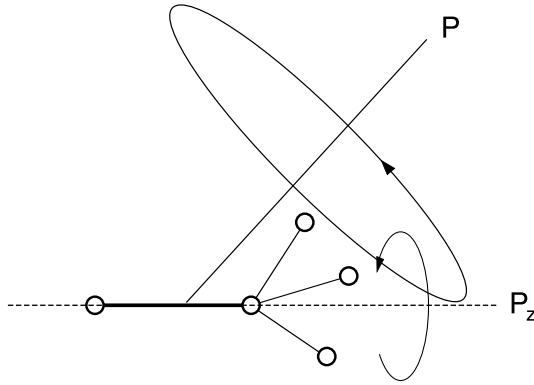
Figure 1: Classical motion of a symmetric rotor (adapted from Townes & Schawlow 1955). The dipole moment is parallel to the unique principal axis P_z, which itself precesses about the total angular momentum vector P.

2.2.1 Selection rules

Selection rules imposed by quantum mechanics and conservation principles mean that not all transitions between energy levels are allowed. Symmetric rotors have no dipole moment perpendicular to the axis of symmetry, hence radiation cannot change the rotational state around the principal axis, and $\Delta K = 0$. The dipole moment lies along the principal axis of the rotor P_z, as shown in Figure 1, which itself precesses about the total angular momentum, P. Conservation of angular momentum dictates that the change in J when a photon is emitted or absorbed must be ± 1. In the absence of other factors it can be shown that there is equal probability of any particular transition with $\Delta J = \pm 1$. If distortion of the molecule through centrifugal stretching is neglected, the frequencies observed for any $\Delta J = \pm 1$ transition do not depend on the value of K and are given by

$$\nu = 2B(J + 1). \tag{8}$$

2.2.2 Centripetal distortion

Molecules are not rigid rotors. Atoms feel the effect of centripetal forces which tend to distort the geometry of the molecule. The effect is to stretch the bonds, leading to a change in the value of I and therefore a change in the value of the rotation constant B. The resultant change in the energy levels is empirically modelled by centripetal distortion constants (D_J, D_K, D_{JK}) and Equation 5 becomes

$$E_{J,K} = h[BJ(J + 1) + (A - B)K^2 - D_J J^2 (J + 1)^2 - D_{JK} J(J + 1)K^2 - D_K K^4]. \tag{9}$$

The frequency of a rotational transition $J \to J + 1, \Delta K = 0$ is then

$$\nu = 2(J + 1)(B - D_{JK}K^2) - 4D_J(J + 1)^3. \tag{10}$$

For a particular $J+1 \to J$ transition, spectral lines due to different K values will be shifted in frequency with respect to each other, giving rise to a 'K-ladder' spectrum. The distortion constants, D_J, D_K and D_{JK}, are very small compared to the rotational constants A and B, so the shift is on the order of a few MHz at 110 GHz. It is this property which makes symmetric tops a good observational probe, as several K-components may be observed in the same bandpass and relative calibration is assured. Figure 2 shows the energy level diagram for the symmetric rotor CH_3CN and the observed spectrum of the J=(5→4) K-ladder in the source G0.55−0.85.
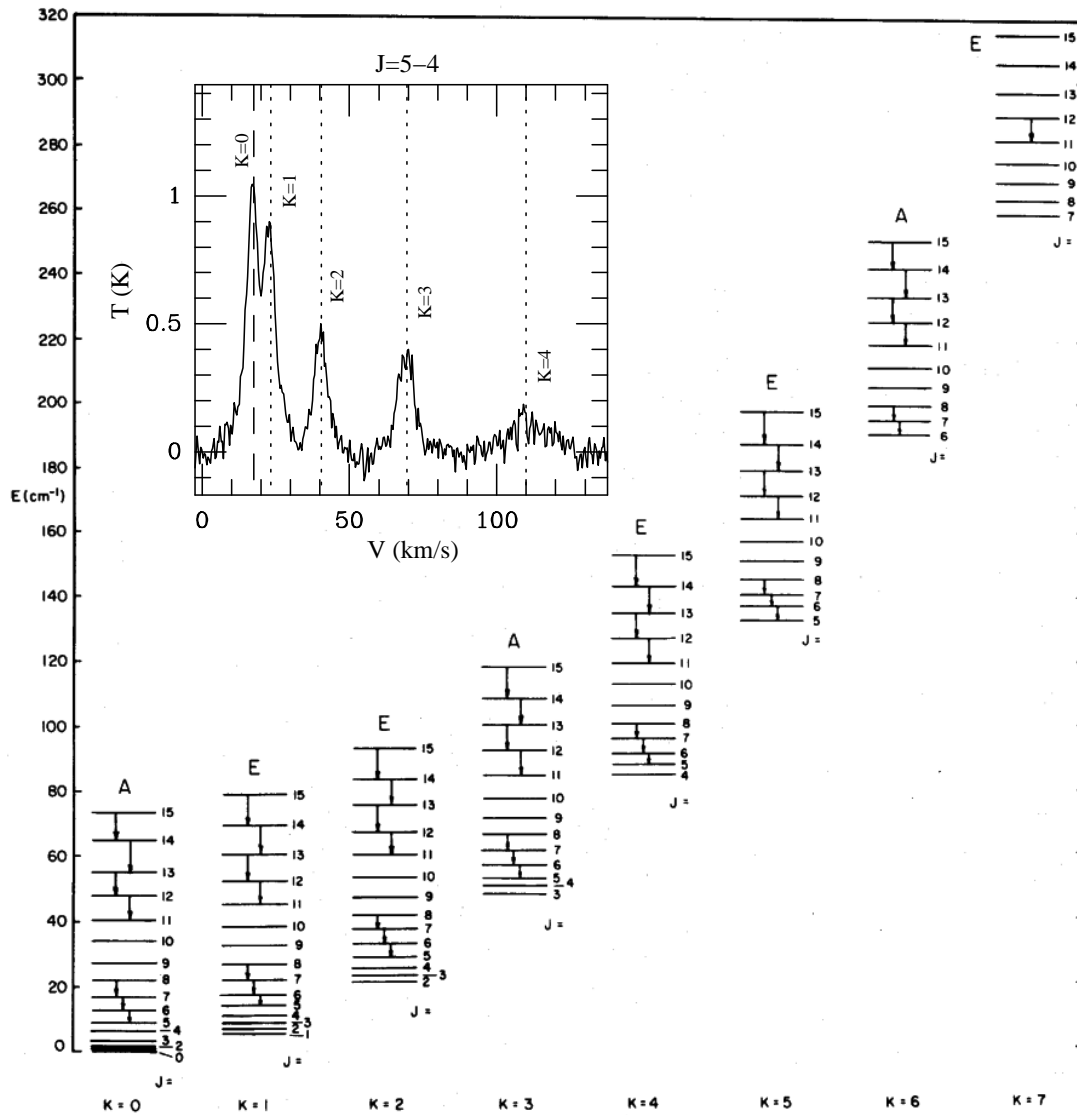
Figure 2: Energy level diagram for the symmetric rotor CH$_3$CN (taken from Loren & Mundy 1984). Energy levels with the same value for K are grouped into 'K-ladders' terminating in the J = K level. Radiative transitions are forbidden between K-ladders so collisions alone are responsible for excitation and under LTE conditions the relative level populations are governed by a Boltzmann distribution. *Inset*: The resultant spectrum in the J = 5→4 K-ladder in the source G0.55−0.85.

2.2.3 Permanent dipole moment

The value of the permanent dipole moment μ determines the effectiveness of an electric field in exerting a torque on a rotating molecule, or in inducing a transition between states J,M and J′,M′, where M = M′ is the magnetic quantum number. If the electric is field polarised along a particular axis (e.g. z) the intensity of the emission or absorption of radiation is proportional to $|\mu_z|^2$, where μ_z is the projection of the electric dipole moment onto that axis. μ_z is known as a dipole moment matrix element. For unpolarised radiation

$$\mathrm{I_{peak}} \propto |\mu_{ij}|^2 = \sum_{M'} |\mu_c(JMJ'M')|^2 + |\mu_y(JMJ'M')|^2 + |\mu_z(JMJ'M')|^2. \tag{11}$$

For any initial state J,K,M it can be shown (see Townes & Schawlow 1955) that

$$|\mu_{ij}|^2 = \mu^2 \frac{(J+1)^2 - K^2}{(J+1)(2J+1)} \quad \text{for the transition } J+1 \leftarrow J, \, K \leftarrow K, \tag{12}$$

$$|\mu_{ij}|^2 = \mu^2 \frac{(J+1)^2 - K^2}{(J+1)(2J+3)} \quad \text{for the transition } J+1 \rightarrow J, \, K \rightarrow K, \tag{13}$$

$$|\mu_{ij}|^2 = \mu^2 \frac{K^2}{J(2J+1)} \quad \text{for the transition } J \leftarrow J, \, K \leftarrow K. \tag{14}$$

The value of μ above is the permanent dipole moment of the molecule, usually quoted in Debyes. In SI units, one Debye = $3.2225641 \times 10^{-30}$ coulomb metres.

2.2.4 Degeneracy of rotational levels

If two or more levels coincide in energy, transitions involving these levels will give rise to overlapping spectral lines. The total angular momentum J may be oriented in space $2J+1$ different ways, corresponding to the different values of the magnetic quantum number M = $0, \ldots \pm J$. Thus the energy of any J level is degenerate by a factor $g_u = 2J + 1$. For symmetric tops, K levels greater than zero are doubly degenerate, as the $-K$ and $+K$ levels have the same energy. Symmetric tops with tri-fold symmetry (e.g., CH_3CN, NH_3) also have a degeneracy due to quantum mechanical symmetry considerations associated with the spins on the three identical atoms. The degeneracy, $S(I, K)$ due to spin and K degeneracy is given by:

$$S(I, K) = 2(4I^2 + 4I + 3) \qquad \text{For K = 3n, n = 1, 2, \ldots} \tag{15}$$
$$S(I, K) = (4I^2 + 4I + 3) \qquad \text{For K = 0} \tag{16}$$
$$S(I, K) = 2(4I^2 + 4I) \qquad \text{For K} \neq \text{3n, n = 1, 2, \ldots} \tag{17}$$

where I is the spin of the identical atoms, which in the case of hydrogen is $\frac{1}{2}$. The total degeneracy of any J,K level is then given by $g_u S(I, K)$.

2.2.5 Population in energy levels

In an ensemble of molecules, the number of molecules at a particular rotational energy will be governed by the Boltzmann Distribution

$$\frac{n_J}{n_0} = \frac{g_J}{g_0} e^{-(E_J - E_0)/kT_{ex}} \tag{18}$$

where n_0 is the number density of molecules in the lowest rotational state (J=0) and n_J is the number density of molecules in the Jth level. T_{ex} is defined as the *excitation temperature*, and will be

A) Boltzmann relation without degeneracy
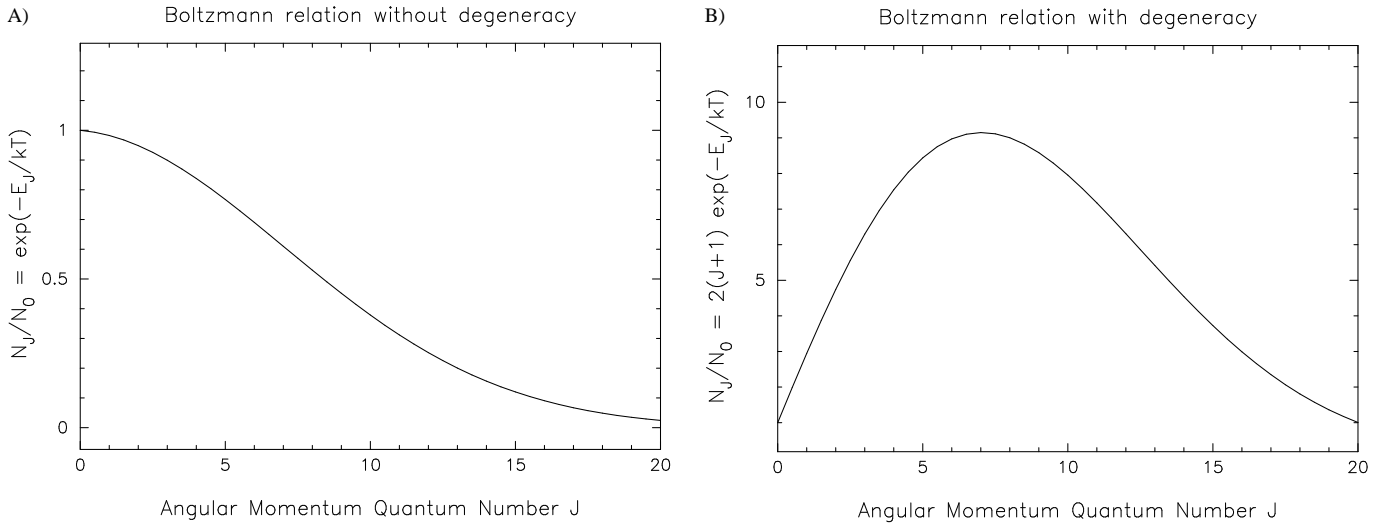
B) Boltzmann relation with degeneracy

Figure 3: The relative population as a function of J for a linear molecule, in this case HCO^+ at $50\,K$. Panel A shows the Boltzmann distribution without taking into account degeneracy. The number density of molecules in higher J levels decreases exponentially. Panel B shows the Boltzmann distribution including a factor of 2J+1 degeneracy. The $J = 7$ level contains the highest population of molecules. As the temperature increases the peak of the curve moves to higher J values.

equal to the kinetic temperature under conditions of local thermal equilibrium (LTE). For a given temperature the number of molecules decreases exponentially with increasing J (Figure 3-A). As the temperature is increased the curve becomes shallower and the higher J levels are populated with greater numbers of molecules. However, as the total degeneracy increases with J, the population curve has the form of Figure 3-B.

The parameter of interest to astronomers is often the total number density of molecules, n, which is given by the sum of the number density of molecules in all states

$$n = \sum_{i=0}^{\infty} n_i. \tag{19}$$

If the energy levels are populated according to the Boltzmann Distribution the total number density of molecules may be inferred from the population in one energy level. By combining Equations 18 and 19 we find

$$n = n_0 \sum_{i=0}^{\infty} \frac{n_i}{n_0} = n_0 \sum_{i=0}^{\infty} \frac{g_i}{g_0} e^{-E_i/kT} = \frac{n_0}{g_0} e^{E_0/kT} Q(T) \tag{20}$$

where $Q(T_{ex})$ is the partition function, a sum over all energy states that normalises the distribution, and is given by

$$Q(T_{ex}) = \sum_i g_i e^{-E_i/kT_{ex}}. \tag{21}$$

2.2.6 Total intensity in a rotational molecular transition

In summary, the intensity of a $J \rightarrow J-1, K$ rotational transition is proportional to the permanent dipole moment μ, the degeneracy of the upper energy level g_u, the number density of emitting molecules n and the excitation temperature of the gas T_{ex} as follows:

$$Intensity \propto \frac{|\mu^2|\, n\, g_u\, S(I, K)\, e^{-(E_u - E_l)/kT_{ex}}}{Q(T_{ex})}. \tag{22}$$

Derivation of the full formula requires a consideration of radiation transport through a medium, which will be presented in Section 3.

2.2.7 Spectral line profiles

Spectral lines are not discrete and are spread out over a finite frequency space. The following mechanisms account for the broadening of a line profile.

Natural broadening is the term given to the intrinsic width of the line, described by a Lorentzian profile. In an ensemble of emitting molecules the Uncertainty principle ($\Delta E \, \Delta t \approx \hbar$) causes variations in the lifetime of an excited state. The effect introduces an uncertainty in the energy level, leading to a spread in the frequency of the emitted or absorbed radiation.

The proximity of other molecules affects the radiation emitted by an individual molecule. **Pressure broadening** occurs when collisions interrupt the emission process, or when the energy levels in the emitting molecule are modified by the presence of other nearby molecules. The magnitude of the effects depend on both the temperature and the density of the gas.

Doppler broadening occurs due to the chaotic motion of the observed molecules in random directions. The resultant Doppler shifts produce a further spread in the frequency of the observed line.

Thermal Doppler broadening is the specific Doppler broadening due to the thermal motions of the molecules. Pure thermal broadening results in a Gaussian line shape with a full-width half-maximum (FWHM) given by

$$\Delta \nu_{\mathrm{FWHM}} = 2 \sqrt{\ln(2)} \, \frac{\nu_0}{c} \sqrt{\frac{2kT_{\mathrm{kin}}}{m}}, \tag{23}$$

where ν_0 is the central frequency and m is the mass of the molecule in kilogrammes.

Large scale collective motions of groups of molecules can also contribute significantly to the broadening of the line profile. This **turbulent Doppler broadening** is described by

$$\Delta \nu_{\mathrm{FWHM}} = 2 \sqrt{\ln(2)} \, \frac{\nu_0}{c} \sqrt{\frac{2kT_{\mathrm{kin}}}{m} + V_{\mathrm{t}}^2}, \tag{24}$$

where V_{t}^2 is a constant called the micro-turbulent velocity.

The gas in cold ($<15\,\mathrm{K}$) quiescent clouds is usually not affected by turbulent motions. In such regions the line profile is dominated by thermal broadening and Equation 23 predicts FWHM linewidths of $\lesssim 0.5\,\mathrm{km\,s^{-1}}$. In molecular clouds forming massive stars linewidths of $>3\,\mathrm{km\,s^{-1}}$ are common and turbulence is the dominant broadening mechanism.

During the analysis of spectral line data Gaussian line profiles are often assumed. The normalised Gaussian line profile is given by:

$$\phi(\nu) = \frac{\sqrt{4 \ln 2}}{\Delta\nu \sqrt{\pi}} \, e^{-4 \ln 2 \left(\frac{\nu}{\Delta\nu}\right)^2}, \tag{25}$$

where ν is the frequency and $\Delta\nu$ is the 1-σ linewidth in frequency units. $\Delta\nu$ is related to the FWHM linewidth via $\Delta\nu = \Delta\nu_{\mathrm{FWHM}}/(2\sqrt{2\ln 2})$ and the area under a Gaussian curve (i.e., the integrated intensity) may be found from

$$\mathrm{Area} = \frac{2\sqrt{\ln 2}}{\sqrt{\pi}} \times \Delta \nu_{\mathrm{FWHM}} \times \mathrm{Height}. \tag{26}$$

2.3 Molecular excitation and Einstein coefficients

Consider an ensemble of molecules with only two energy levels E_u and E_l, bathed in a radiation field of specific intensity I_ν. The population in both levels is governed by the interaction of the system with external radiation and particles. Radiative transitions between the levels are conveniently described by the Einstein coefficients, which are defined as:

- A_{ul} = Probability of spontaneous radiative decay from the upper to the lower energy level (s^{-1}).

- $\bar{I} B_{ul}$ = Probability of stimulated emission from the upper to the lower energy level.

- $\bar{I} B_{lu}$ = Probability of photon absorption leading to a transition from the lower to upper energy level.

$\bar{I}$ is the average intensity of the external radiation field. The Einstein coefficients are intrinsic properties of the particular transition, and are related to the molecular properties via

$$A_{ul} = \frac{16\,\pi^3\,\nu^3}{3\,\epsilon_0\,h\,c^3}\,|\mu^2| \tag{27}$$

where $|\mu^2|$ is the dipole matrix element for the transition given by one of Equations $12-14$, ϵ_0 is the permittivity of free space, and ν is the frequency of the transition. The Einstein A and B coefficients are related through

$$B_{ul} = \frac{c^2}{2h\nu^3}\,A_{ul} \qquad \text{and} \qquad B_{lu}\,g_l = B_{ul}\,g_u. \tag{28}$$

The Einstein coefficients describe interactions between the system and external radiation, however, collisions can also cause excitation and de-excitation. Collisional coefficients are defined according to:

- $C_{ul} = n_{H_2}\,\gamma_{ul}$ = Rate of collision induced transitions from upper to lower level (in molecules s^{-1}).

- $C_{lu} = n_{H_2}\,\gamma_{lu}$ = Rate of collision induced transitions from lower to upper level (in molecules s^{-1}).

where n_{H_2} is the H_2 number density and γ_{ul} and γ_{lu} are the coefficients for downward and upward collisions, respectively (in molecules s^{-1} H_2-molecules^{-1}). We assume here that H_2 molecules are the dominant collisional partner and $\gamma = \gamma_{H_2}$. In the steady state the number of molecules in upper and lower levels remain constant, therefore:

$$n_u\,[A_{ul} + B_{ul}\,\bar{I}_\nu + C_{ul}] = n_l\,[B_{lu}\,\bar{I}_\nu + C_{lu}], \tag{29}$$

where n_u is the number density of molecules in the upper state and n_l is the number density of molecules in the lower state. Assuming LTE conditions, (and therefore a Boltzmann population distribution), an excitation temperature, T_{ex}, describing the ratio of the level populations is defined from Equation 18 (repeated here):

$$\frac{n_u}{n_l} = \frac{g_u}{g_l}\,e^{-(E_u - E_l)/k\,T_{ex}}.$$

Considering only collisions, ($n_l\,C_{lu} = n_u\,C_{ul}$), and applying Equation 18 we find a Boltzmann relation for the ratio of the collision rates:

$$\frac{C_{lu}}{C_{ul}} = \frac{g_u}{g_l}\,e^{-(E_u - E_l)/k\,T_{kin}}, \tag{30}$$

called the 'detailed balance' condition. Although we derived this relation assuming the radiation field was negligible, it must always hold since it depends only on molecular parameters. By combining Equations 29 and 18 we arrive at an expression for the excitation temperature:

$$\frac{n_u}{n_l} = \frac{g_u}{g_l} \, e^{-(E_u - E_l)/k \, T_{ex}} = \frac{B_{lu} \bar{I}_\nu + C_{lu}}{A_{ul} + B_{ul} \bar{I}_\nu + C_{ul}} \tag{31}$$

If the radiation originates from a blackbody (e.g. the Cosmic Microwave Background) with a temperature T_{bg}, then $\bar{I}_\nu$ will be given by the Planck radiation law

$$\bar{I}_\nu = B_\nu(T_{bg}) = \frac{2h\nu^3}{c^2} \, J_\nu(T), \tag{32}$$

with $J_\nu(T) = (e^{(E_u - E_l)/kT_{bg}} - 1)^{-1}$. Using Equation 30 and substituting for $\bar{I}_\nu$ in Equation 31 we find

$$e^{(E_u - E_l)/k \, T_{ex}} = \frac{A_{ul}[1 + J_\nu(T_{bg})] + C_{ul}}{A_{ul}J_\nu(T_{bg}) + C_{ul} \, e^{-E_u/k \, T_{kin}}}, \tag{33}$$

which relates the excitation temperature to the kinetic temperature in a gas bathed in a radiation field. Consider two limiting cases:

Collisions Unimportant: Radiation dominates the excitation, collisional terms are negligible and may be discarded. The population is in equilibrium with the background radiation field and

$$T_{ex} = T_{bg}. \tag{34}$$

Collisions Dominate: Excitation takes place mainly due to collisions and the radiative terms may be discarded. The population is in thermal equilibrium and

$$T_{ex} = T_{kin}. \tag{35}$$

A useful quantity to define is the *critical density* of H_2 at which downward collisional processes equal downward radiative processes. It is taken to be a measure of the density necessary for collisional excitation to be effective. In the steady state equation the downward terms are:

$$A_{ul} + A_{ul}J_\nu(T_{bg}) = n_{H_2}\gamma_{ul}$$

and the critical density is defined as:

$$n_{crit} = \frac{A_{ul}(1 + J(T_{bg}))}{\gamma_{ul}} \approx \frac{A_{ul}}{\gamma_{ul}} \tag{36}$$

At densities lower than n_{crit}, collisions are too infrequent to excite the gas and under LTE conditions a spectral line will not be visible against the background radiation. The value of A_{ul} increases with ν_{ul}^3 (Equation 27), so higher frequency transitions trace increasingly dense gas.

3 Radiative transfer in an isothermal medium

Having laid the ground rules governing molecular excitation in an ensemble of molecules, we must now consider how the spectral lines are processed as they pass through the intervening gas and dust to reach the observer. The following description is equally valid for continuum radiation, such as thermal radiation due to warm dust, or free-free emission from a H_{II} region.
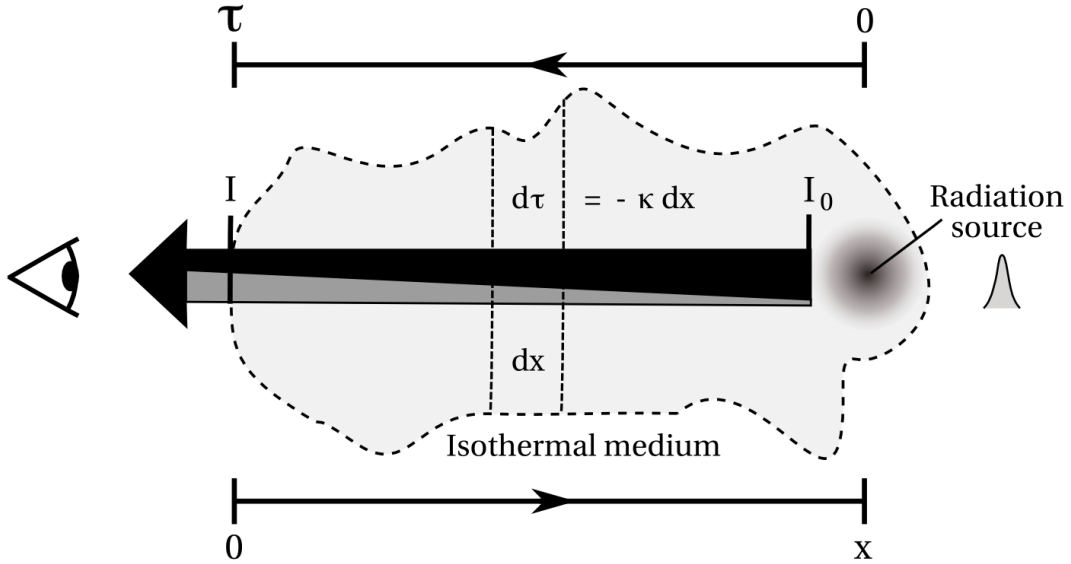
Figure 4: For a radiating source embedded in a molecular cloud the intensity measured by an external observer will be the sum of the initial intensity I_0, attenuated by the intervening medium (black bar), and the self-attenuated emission from the medium (grey bar). The change in intensity over any interval dx is described by the radiative transfer equation (Equation 37) in terms of κ and ϵ, the absorption and emission coefficients of the medium.

3.1 The equation of radiative transfer

The change in the intensity of radiation as it passes through an isothermal medium (e.g. a molecular cloud, Figure 4) is described by the radiative transfer equation:

$$\frac{dI_\nu}{ds} = -\kappa_\nu I_\nu + \epsilon_\nu, \tag{37}$$

where I_ν is the specific intensity of the radiation, κ_ν is the absorption coefficient and ϵ_ν is the specific intensity of radiation emitted by the medium. The absorption and emission coefficients in the radiative transfer equation can be expressed in terms of the Einstein coefficients:

$$\epsilon_\nu = \frac{h\nu_{ul}}{4\pi} n_u A_{ul} \phi(\nu), \tag{38}$$

$$\kappa_\nu = \frac{h\nu_{ul}}{4\pi} (n_l B_{lu} - n_u B_{ul}) \phi(\nu), \tag{39}$$

where $\phi(\nu)$ is a normalised line profile, usually taken to be Gaussian in form. Equation 37 may also be expressed in terms of optical depth τ_ν, defined as $\tau_\nu = -\kappa_\nu ds$, giving

$$\frac{dI_\nu}{d\tau_\nu} = I_\nu - \frac{\epsilon_\nu}{\kappa_\nu} = I_\nu - S_\nu, \tag{40}$$

where $\epsilon_\nu / \kappa_\nu$ completely describes the properties of the medium and is known as the source function, S_ν.

The radiative transfer equation may be solved to obtain an expression for observed intensity, I_ν, as a function of distance s:

$$I_{\nu,s} = I_{\nu,0} e^{-\tau_\nu} + S_\nu (1 - e^{-\tau_\nu}). \tag{41}$$

This is the general solution to the radiative transfer equation assuming an isothermal, homogeneous medium. The intensity of the detected radiation is the sum of the attenuated radiation from the source, $I_{\nu,0} e^{-\tau_\nu}$, and the self attenuated radiation emitted by the medium, $S_\nu (1 - e^{-\tau_\nu})$.

3.2 Brightness temperature and the detection equation

If the source of radiation is assumed to be a blackbody then the source function S_ν will be described by Equation 32, Planck's radiation law. At low frequencies when $h\nu \ll kT$ the Planck function is well approximated by the Rayleigh-Jeans Law:

$$S_\nu = B_\nu(T_R) \approx \frac{2k\nu^2 T_R}{c^2}, \tag{42}$$

where T_R is the radiation temperature of the source. A brightness temperature T_b is defined such that

$$T_b = \frac{c^2}{2k\nu^2} B_\nu(T_R) = \frac{h\nu}{k} J_\nu(T_R), \tag{43}$$

with $J_\nu(T) = (e^{(E_u - E_l)/kT} - 1)^{-1}$ as before. Equation 41 may be expressed in terms of brightness temperatures:

$$T_b = \frac{h\nu}{k} J_\nu(T_{bg}) e^{-\tau_\nu} + \frac{h\nu}{k} J_\nu(T_s)(1 - e^{-\tau_\nu}), \tag{44}$$

where T_{bg} is the temperature of the background radiation field and T_s is the radiation temperature of the source. During position or frequency switched observations the excess brightness temperature above a background (e.g., the cosmic microwave background) is measured and Equation 44 becomes

$$T_b = \frac{h\nu}{k} [J_\nu(T_s) - J_\nu(T_{bg})](1 - e^{-\tau_\nu}). \tag{45}$$

This is known as the detection equation as it relates the brightness temperature measured at the telescope to the thermodynamic temperature of the source. Two special cases occur when the medium is optically thin ($\tau \ll 1$) or optically thick ($\tau \gg 1$):

Optically Thin Emission:

$$T_b = \frac{h\nu}{k} [J_\nu(T_s) - J_\nu(T_{bg})]\tau_\nu \tag{46}$$

Optically Thick Emission:

$$T_b = \frac{h\nu}{k} [J_\nu(T_s) - J_\nu(T_{bg})] \tag{47}$$

4 Physical parameters from observations

Of primary interest to the astronomer are the physical conditions such as kinetic temperature, density and abundance which give rise to the spectral lines. Under optically thick conditions the brightness of a spectral line saturates at the excitation temperature, which under LTE conditions is proportional to the kinetic temperature (Equation 35). Under optically thin conditions the intensity under a spectral line is proportional to the number of molecules emitting and their excitation temperature (Equation 22). In this case the total number density of molecules emitting in the beam (the column density) may be found if the excitation temperature is known. Traditionally, the excitation temperature is found from observations of generally optically thick transitions (e.g. $CO\,1-0$) and the column density is found from a generally optically thin isotopomer (e.g. $C^{18}O\,1-0$), assuming the same excitation temperature.

4.1 Kinetic temperature from optically thick transitions

If the emission is optically thick then Equation 47 and the Planck functions allows us to determine the source temperature as follows

$$\frac{1}{J_\nu(T_s)} = e^{h\nu/kT_{kin}} - 1 = \frac{(h\nu/k)}{T_b + \frac{h\nu}{k} J_\nu(T_{bg})}.$$

If local thermal equilibrium conditions apply then $T_s = T_{kin}$ so

$$T_{kin} = T_s = \frac{h\nu}{k} \left[\ln \left(1 + \frac{(h\nu/k)}{T_b + \frac{h\nu}{k} J_\nu(T_{bg})} \right) \right]^{-1}. \tag{48}$$

This equation gives the kinetic temperature of the gas if the line is optically thick.

4.2 Column density from optically thin transitions

Expanding the definition of optical depth, τ_ν, using Equations 39 and 28:

$$\tau_\nu = -\kappa_\nu \, ds \quad = \quad \frac{c^2}{8\pi\nu^2} \, A_{ul} \, (n_l \, \frac{g_u}{g_l} - n_u) \, \phi(\nu) \, ds,$$

and substituting the Boltzmann Equation (18) for g_u/g_l we find:

$$\tau_\nu = \frac{c^2}{8\pi\nu^2} \, A_{ul} \, n_u \, (e^{h\nu_{ul}/kT_{ul}} - 1) \, \phi(\nu) \, ds. \tag{49}$$

Now integrate along the line of sight to obtain

$$\tau_\nu = \frac{c^2}{8\pi\nu^2} \, A_{ul} \, N_u \, (e^{h\nu_{ul}/kT_{ul}} - 1) \, \phi(\nu), \tag{50}$$

where $N_u = \int n_u ds$ is the column density of molecules in the upper state and $\phi(\nu)$ is the normalised line profile, usually taken to be a Gaussian.

Returning to the detection equation (45), and assuming emission from background is negligible, we find

$$T_b = \frac{h\nu}{k} \, J_\nu(T_{ex}) \, (1 - e^{-\tau_\nu}). \tag{51}$$

As a convenience we will multiply by τ/τ and substitute the full expression for optical depth (Equation 50):

$$T_b = \left(\frac{h\nu}{k} \, J_\nu(T_{ex}) \right) \left(\frac{1 - e^{-\tau_\nu}}{\tau_\nu} \right) \left(\frac{c^2}{8\pi\nu^2} \, A_{ul} \, N_u \, (e^{E_{ul}/kT_{ul}} - 1) \, \phi(\nu) \right)$$

$$= \frac{hc^2}{8k\pi\nu} A_{ul} \, N_u \left(\frac{1 - e^{-\tau_\nu}}{\tau_\nu} \right) \phi(\nu).$$

Then integrate over the full width of the line (normalised to 1):

$$\int_{-\infty}^{\infty} T_b \, d\nu = \frac{\nu}{c} \int_{-\infty}^{\infty} T_b \, dv = \frac{hc^3}{8k\pi\nu^2} \, A_{ul} \, N_u \left(\frac{1 - e^{-\tau_\nu}}{\tau_\nu} \right) \int_{-\infty}^{\infty} \phi(\nu) \, d\nu$$

to find the general relation for the column density of molecules in the upper energy level:

$$N_u = \frac{8k\pi\nu^2}{A_{ul}hc^3} \int_{-\infty}^{\infty} T_b \, dv \left(\frac{\tau_\nu}{1 - e^{-\tau_\nu}} \right). \tag{52}$$

Here $\int T_b \, dv$ is the integrated intensity of the spectral line in $km\,s^{-1}$. In the optically thin case the term $(1 - e^{-\tau_\nu})/\tau_\nu$ is approximately equal to one and

$$N_u = \frac{8k\pi\nu^2}{A_{ul}hc^3} \int_{-\infty}^{\infty} T_b \, dv. \tag{53}$$

This equation gives the column density in the *upper state* assuming optically thin conditions. To find the total column density from Equations 52 or 53 we must assume all the energy levels are populated according to a Boltzmann distribution characterised by a single temperature, T_{ex}. The total column density may then be found from Equations 20 and 21, repeated here:

$$N = \frac{N_u}{g_u} \, e^{E_u/kT} \, Q(T_{ex}) \qquad \text{and} \qquad Q(T_{ex}) = \sum_i g_i \, e^{-E_i/kT_{ex}}.$$

4.3 The rotational diagram

In many instances it is not practical or possible to find an optically thick tracer to measure the excitation temperature and an optically thin tracer to measure the column density. Fortunately, there is a better way to measure both simultaneously through the analysis of the excitation of asymmetric molecules. The *rotation diagram* method simultaneously yields the excitation temperature T_{ex} and total column density N, assuming LTE and optically thin transitions.

Equation 20 relates the upper state column density to the total column density, assuming Boltzmann statistics. Rearranging and taking the natural log of both sides we find

$$\ln\left(\frac{N_u}{g_u}\right) = \ln\left(\frac{N}{Q(T)}\right) - \frac{E_u}{kT_{ex}}. \tag{54}$$

The column density in the upper level, N_u may be found from the integrated intensity under the spectral line, ($\int_{-\infty}^{\infty} T_b \, dv$), through Equation 53. If several transitions have been measured, a straight line through a plot of $\ln(N_u/g_u)$ versus E_u/k will have a slope of $1/T_{ex}$ and a y-intercept of $\ln[N/Q(T)]$. Temperatures found through this method are referred to as rotational temperatures ($T_{ex} = T_{rot}$).

Symmetric tops lend themselves well to this approach as multiple $(J+1 \rightarrow J, K)$ transitions may be observed in a single bandpass. Radiative transitions are forbidden between K levels, therefore the relative population in the K levels is determined only by collisions and T_{rot} will be equal to the kinetic temperature.

5 Case study: NH₃, the molecular thermometer

Ammonia (NH₃) is a symmetric rotor that constitutes an ideal probe of the temperatures and densities in molecular clouds. The spectrum of NH₃ is distinguished from other symmetric tops as it is split into five 'hyperfine groups' - a main group and two pairs of satellite lines. The optical depth may be determined directly from the intensity ratios of the satellite lines, facilitating the calculation of rotational temperatures and column densities without making the assumption of optically thin conditions. In addition, the collisional excitation of NH₃ has been extensively modelled allowing the accurate conversion of rotational temperatures to kinetic temperatures. In the following sections we outline the theory necessary to understand the form of the NH₃ inversion spectrum and describe the modified rotational diagram analysis used to calculate kinetic temperatures and column densities.

5.1 The spectrum of NH₃

The rich spectrum of NH₃ is a result of interactions between vibrational and rotational modes, and the internal electronic structure of the molecule. We will examine the contribution from each mode in turn, leading to an explanation for the form of the observed spectrum.

Inversion

NH₃ is a trigonal pyramid with three identical N–H bonds. It is a member of a unique class of molecules which vibrate in an 'inversion' mode (Kukolich, 1967). Figure 5-a illustrates the structure of NH₃. The potential experienced by the nitrogen atom is that of a double well, with one well on either side of the plane defined by the three hydrogen atoms (Figure 5-b). Classically, the nitrogen atom is confined to a single well, as in the ground state it does not have enough energy to overcome the central barrier. However, quantum theory allows the nitrogen to 'tunnel' through the barrier and it has a non-zero probability of being found in the opposite well after a finite time.
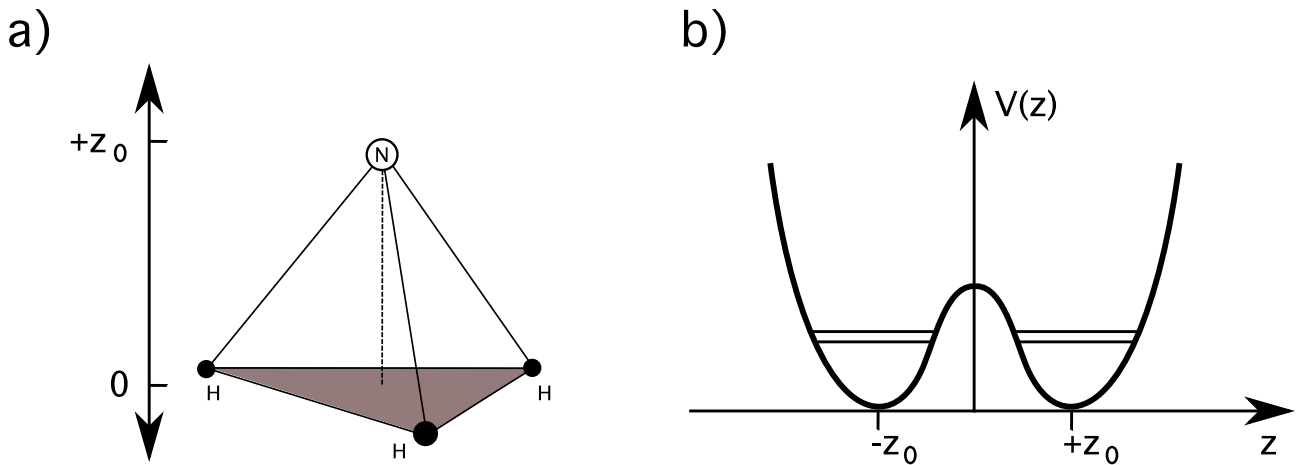
Figure 5:   a) The trigonal-pyramid structure of NH_3. The Nitrogen atom can quantum mechanically 'tunnel' through the plane of the Hydrogen atoms, giving rise to the inversion transitions. b) The double-well potential experienced by the nitrogen atom due to Coulomb repulsion by the three hydrogen atoms.
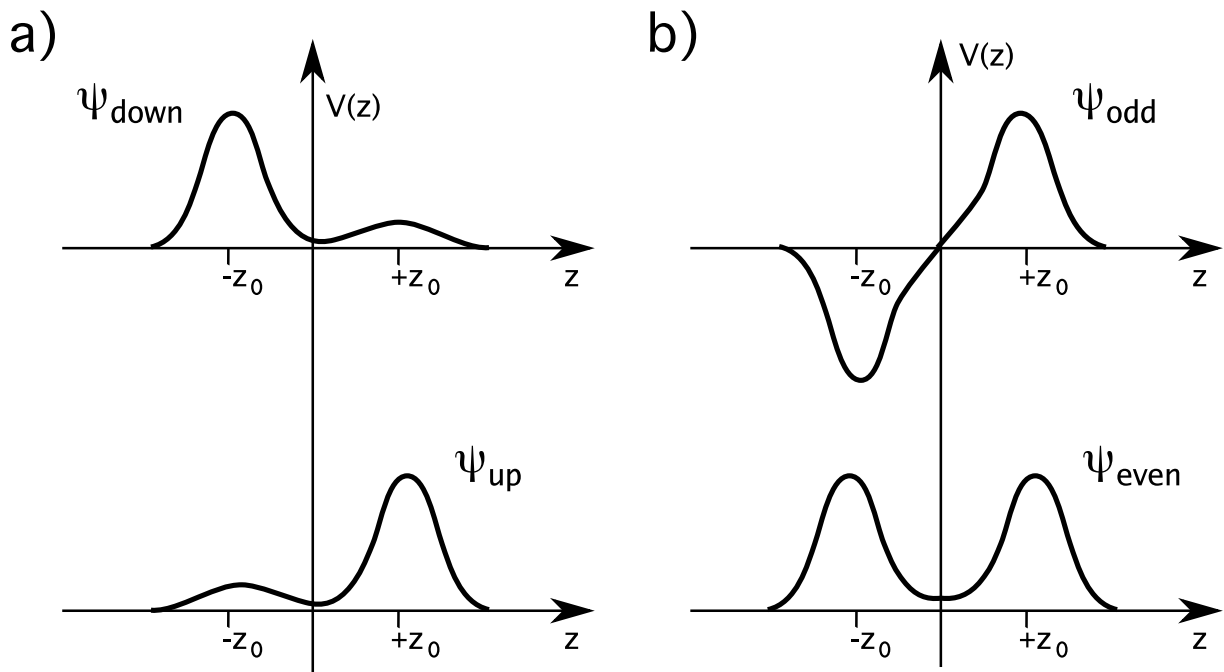

Figure 6: a) Individual solutions to the Schroedinger equation for a double well potential. b) Eigenfunctions for the double well potential with a finite barrier.

Inversion energies

The wavefunctions describing the solution to the Schroedinger equation for a double well are illustrated in Figure 6a. ψ_{up} and ψ_{down} represent the wavefunctions when the nitrogen atom is predominantly localised to the $+z$ and $-z$ sides of the plane, respectively. The full solution is formed from linear combinations of ψ_{up} and ψ_{down} satisfying the requirement $\psi(z) = \pm\psi(-z)$. This is necessary because the wavefunction must have identical forms in both wells under transformation in Cartesian coordinates. Two solutions are defined:

$$\psi_{\mathrm{odd}} = \left(\frac{1}{\sqrt{2}}\right)(\psi_{\mathrm{up}} - \psi_{\mathrm{down}}) \qquad \text{and} \qquad \psi_{\mathrm{even}} = \left(\frac{1}{\sqrt{2}}\right)(\psi_{\mathrm{up}} + \psi_{\mathrm{down}}).$$

These wavefunctions are illustrated in Figure 6b. The complete expressions for ψ_{odd} and ψ_{even} in the steady state are given by

$$\psi_{\mathrm{odd}}(z,t) = \psi_{\mathrm{odd}}(z)\,e^{-iE_1 t/\hbar} \qquad \text{and} \qquad \psi_{\mathrm{even}}(z,t) = \psi_{\mathrm{even}}(z)\,e^{-iE_2 t/\hbar},$$

where E_1 and E_2 are the energies of the ψ_{odd} and ψ_{even} wavefunctions. $E_1 > E_2$ as can be seen by decreasing the height of the potential barrier. As the shape of the potential approaches that of a single well the ψ_{odd} and ψ_{even} wavefunctions approach the first and second vibrational states, respectively, of a linear molecule. For NH_3 in the ground vibrational state, the inversion transition between E_1 and E_2 corresponds to a frequency $\nu_0 = 23.8\,\mathrm{GHz}$.

Rotation

Centripetal distortion of the molecule leads to a splitting of the inversion transition into multiple lines. The shape of the potential barrier is determined by the separation between the nitrogen atom and the hydrogen atoms. This spacing in turn is dependent on the quantised rotational state of the molecule. Rotation about the principal axis ($J>0$, $K=J$) tends to flatten out the pyramid, increasing the distance between the hydrogen atoms. Hence, the potential barrier lowers and the inversion frequency increases. If there is significant angular momentum perpendicular to the principal axis ($J>0$, $K \ll J$) then rotation tends to elongate the pyramid, leading to a higher potential barrier and a decrease in the inversion frequency. The inversion frequency of a J,K level is given by (Townes & Schawlow, 1955)

$$\nu_{\mathrm{inversion}} = \nu_0 - c_1[J(J+1) - K^2] + c_2 K^2, \tag{55}$$

where c_1 and c_1 are positive constants. Quantum symmetry considerations forbid the splitting of any state where $K=0$.

Quadrupole splitting

The nitrogen nucleus has a quadrupole moment resulting from the non-spherical distributions of charge within the nucleus. This quadrupole moment interacts with the electric field of the electrons giving rise to further splitting. Each J,K inversion energy level splits into three levels characterised by the quantised nuclear spin of the nitrogen, $I=1$, and the total angular momentum, $F=I+J$. The following selection rules apply:

$$F = J+1, J, J-1 \qquad \Delta F = 0, \pm 1 \qquad \Delta J = 0, \pm 1 \qquad \Delta I = 0,$$

leading to seven transitions between the ψ_{odd} and ψ_{even} inversion levels. Figure 7 (*top*) illustrates the resultant energy levels for the case of the J,K=(1,1) transition. These transitions lead to the distinctive 5-finger spectrum of NH_3, illustrated in Figure 7 (*bottom*). The central (or main) group is comprised of the transitions with $\Delta F = 0$ and the $\Delta F = \pm 1$ transitions appear as pairs of satellite

Figure 7: (*Top*) Schematic showing the quadrupole and magnetic hyperfine splitting of the NH$_3$ (1,1) inversion spectrum (taken from Rydbeck et al. 1977). (*Bottom*) Typical example of a NH$_3$ (1,1) spectrum showing the main group (centre) and the pairs of satellite lines on either side.

Table 1: Relative intensities of the quadrupole hyperfine lines in the NH_3 spectrum.

Rotational Transition	F-Transition		Relative[α] Intensity	Hyperfine Group	f[β]
J, K=(1,1)	ΔF=0	F=0 → 0	0.0A_1	Main	
		F=1 → 1	6.0A_1	Main	0.502
		F=2 → 2	30.0A_1	Main	
	ΔF=±1	F=1 ↔ 0	8.0A_1	Outer Satellites	0.111
		F=1 ↔ 2	10.0A_1	Inner Satellites	0.139
J, K=(2,2)	ΔF=0	F=1 → 1	54.0A_2	Main	
		F=2 → 2	83.3A_2	Main	0.796
		F=3 → 3	149.7A_2	Main	
	ΔF=±1	F=2 ↔ 1	18.0A_2	Outer Satellites	0.050
		F=2 ↔ 3	10.7A_2	Inner Satellites	0.052

[α]   The relative intensities tabulated here have been calculated from Equations 56, 57 and 58. A_1 and A_2 are normalisation factors chosen so that the total intensity across all hyperfine components is equal to 1. A_1=0.0139 for J, K=(1,1) and A_2=0.0360 for J, K=(2,2).

[β]   Fractional intensity of the line, i.e., the fraction of the total intensity present in the main line or individual satellite lines under optically thin conditions.

lines on either side of the main line. The relative intensities of these transitions may be calculated from

$$F - 1 \rightarrow F: \qquad -\frac{A(J + F + I + 1)(J + F - I)(J - F + I + 1)(J - F - I)}{F} \qquad (56)$$

$$F \rightarrow F: \qquad \frac{A[J(J + 1) + F(F + 1) - I(I + 1)]^2 (2F + I)}{F(F + 1)} \qquad (57)$$

$$F + 1 \rightarrow F: \qquad -\frac{A(J + F + I + 2)(J + F - I + 1)(J - F + I)(J - F - I - 1)}{F + 1} \qquad (58)$$

Values for the J,K=(1,1) and (2,2) transitions are tabulated in Table 1.

Magnetic hyperfine splitting.

Both the nitrogen and hydrogen nuclei have magnetic moments which interact with the magnetic field generated by the rotating molecule. This results in energy shifts much smaller than the quadrupole splitting and the main line and satellites are further split into a total of 18 components. Observations presented here are not capable of resolving these lines (see Figure 7).

Inversion-rotation energy levels

Figure 8 is the energy level diagram for the inversion-rotation states of NH_3 showing the quadrupole hyperfine splitting (from Ho & Townes 1983). Radiative transitions between the K-ladders are normally forbidden by the selection rule ΔK=0, however, interactions between vibrational and rotational motions induce a small dipole moment perpendicular to the rotation axis giving rise to very slow $\Delta k = \pm 3$, K = |k| transitions between K-ladders. Within each K-ladder the upper states (J > K) are called non-metastable because they can decay rapidly down to the lowest 'metastable' states via the
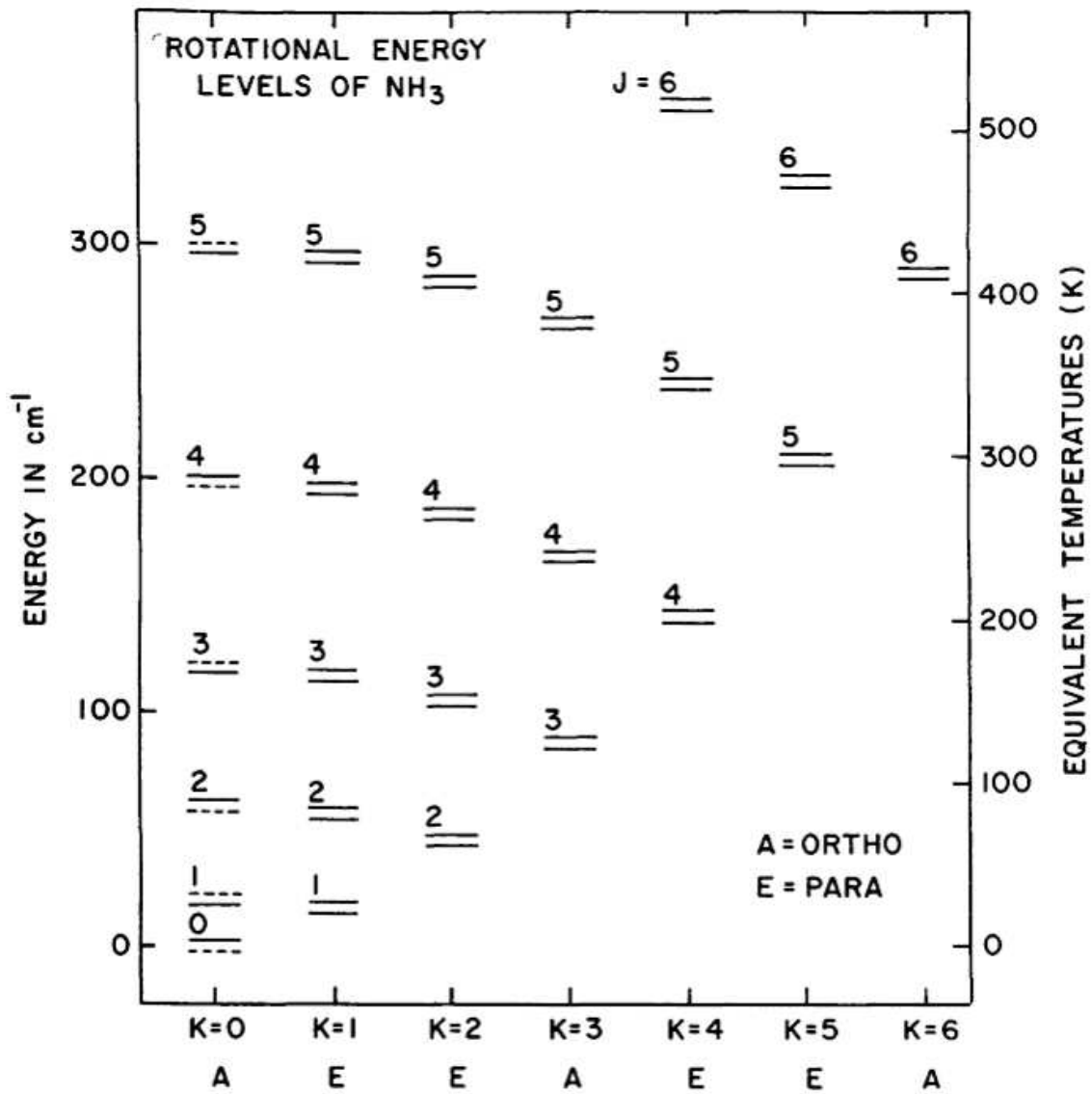
Figure 8: The energy levels for NH$_3$(taken from Ho & Townes 1983).

$\Delta J = 1$ transitions in the far-infrared (Oka et al., 1971). The lowest states in each ladder $(J = K)$ are called the metastable states as they can only decay via the much slower $(10^9 \, \text{s})$ $\Delta k = \pm 3$ transitions (Ho & Townes, 1983). The population in the metastable states thus excited mostly by collisions and should reflect the kinetic temperature of the gas via a Boltzmann distribution.

NH$_3$ is divided into two distinct species based on the orientation of the hydrogen spins. Ortho-NH$_3$ has all H-spins parallel, and gives rise to (K=3n, n=1,2,3,...) levels while Para-NH$_3$ has some H-spins anti-parallel and gives rise to (K≠3n, n=1,2,3,...) levels. Under normal conditions these species do not inter-convert. Ortho-NH$_3$ has twice the statistical weight of para-NH$_3$.

5.2 Modified rotational diagram method

Here we present the modified rotational diagram method used to calculate kinetic temperatures and column densities via a comparison of the NH$_3$(1,1) and (2,2) spectra. This method follows closely to that presented in Ungerechts et al. (1986), who consolidated the methods of Ho et al. (1977), Ungerechts et al. (1980) and Townes et al. (1983).

1: Determine optical depth of the J,K=(1,1) transition

Optical depth as a function of frequency over the NH$_3$ spectrum may be modelled by a sum of five individual Gaussian line profiles

$$\tau(\nu) = \tau^{\text{total}} \times \phi(\nu) \quad = \quad \tau^{\text{total}} \times \sum_{i=1}^{5} f_i \left[\exp \, - \left(\frac{\nu - \nu_0 - \Delta\nu_i}{\Delta\nu} \right) \right], \tag{59}$$

where f_i is the fraction of the total intensity the i$^{\text{th}}$ component (see Table 1), $\Delta\nu_i$ is the frequency offset between i$^{\text{th}}$ component and the central component, ν_0 is the frequency of the central component, and $\Delta\nu$ is the common linewidth. The total optical depth is related to the physical conditions in the gas via Equation 50,

$$\tau^{\text{total}} = \tau^{\text{peak}} = \frac{c^2}{8\pi\nu^2} A_{\text{ul}} N_{\text{u}} (e^{h\nu/kT_{\text{ex}}} - 1) \, \phi^{\text{peak}},$$

where the ϕ^{peak} is the peak height of an unsplit J,K line profile. Assuming a normalised Gaussian profile, this is given by

$$\phi^{\text{peak}} = \frac{\sqrt{4\ln 2}}{\Delta\nu\sqrt{\pi}}. \tag{60}$$

Intensity as a function of frequency may then be modelled by applying $\tau(\nu)$ calculated from Equation 59 to the detection equation (Equation 45):

$$T_{\text{b}}(\nu) = \frac{h\nu}{k} \left[J_\nu(T_{\text{ex}}) - J_\nu(T_{\text{bg}}) \right] (1 - e^{-\tau(\nu)}).$$

A fit of this model profile to the observed spectrum will yield the total optical depth, excitation temperature and linewidth. The NH$_3$(1,1) and NH$_3$(2,2) hyperfine fitting routines in the CLASS[2]. analysis package performs this fit automatically.

Alternatively, optical depth may be found by comparing the peak intensities of the satellites and the main line. From the detection equation we see that

$$\frac{T_{\text{B,main}}}{T_{\text{B,sat}}} = \frac{1 - e^{-\tau_{\text{main}}}}{1 - e^{-\tau_{\text{sat}}}} = \frac{1 - e^{-\tau_{\text{main}}}}{1 - e^{-a_{\text{ms}}\tau_{\text{main}}}}, \tag{61}$$

---

[2]CLASS is a spectral line analysis package within the GILDAS suite of radio-astronomy processing software, which is available at: http://www.iram.fr/IRAMFR/GILDAS/

where 'a$_{ms}$' is the expected ratio of T_{main}/T_{sat} under optically thin conditions. Theoretically, this ratio is found from a$_{ms}$ = f$_{main}$/f$_{sat}$ whose values are presented in column four of Table 1. Equation 61 must be solved numerically for τ_{main}. The total optical depth of the transition is then found from

$$\tau^{total} = \frac{\tau_{main}}{f_{main}}. \tag{62}$$

This method is equally valid for any $J \to J, K = \pm 1, \ldots \pm J$ transition of the NH$_3$ inversion spectrum.

2: Determine optical depth of the J,K=(2,2) transition

In practise, for transitions with $J > 1$ it is often difficult to calculate the optical depth directly from the brightness temperature ratio of satellite to main lines as the signal-to-noise on the weak satellite lines is usually poor. For any (J,K) transition, $\tau_{J,K}$ may be calculated from the ratio of the NH$_3$(J,K) and NH$_3$(1,1) main lines instead, assuming the emission comes from the same gas and the level populations are described by the same excitation temperature. Considering only the main line in each spectrum, Equations 62 and 45 give

$$\tau_{J,K\,main} = \tau_{J,K}^{total} \times f_{J,K\,main} = -\ln\left(1 - \frac{T_{B_{J,K\,main}}}{A_{J,K\,main}}\right), \tag{63}$$

where $A_{J,K\,main} = [J(T_{ex}) - J(T_{bg})]$. In the case of the NH$_3$ (2,2) line we have

$$\tau_{2,2}^{total} = -\frac{1}{f_{2,2\,main}} \ln\left(1 - \frac{T_{B_{2,2\,main}}}{A_{1,1\,main}}\left[\frac{A_{1,1\,main}}{A_{2,2\,main}}\right]\right). \tag{64}$$

For equal excitation temperatures the factor $[A_{1,1,main}/A_{2,2\,main}]$ is approximately 1. From the detection equation we see that $A_{1,1\,main} = T_{B_{1,1,main}}/(1 - e^{-\tau_{1,1\,main}})$ and Equation 64 becomes

$$\tau_{2,2}^{total} = -\frac{1}{f_{2,2\,main}} \ln\left[1 - \frac{T_{B_{2,2\,main}}}{T_{B_{1,1\,main}}}\left(1 - e^{-\tau_{1,1\,main}}\right)\right]. \tag{65}$$

3: Calculate the rotational temperature

A rotational temperature may be defined from Equation 54:

$$\ln\left(\frac{N_u}{g_u}\right) = \ln\left(\frac{N}{Q(T)}\right) - \frac{E_u}{kT_{rot}},$$

where N_u is the column density of molecules in the upper state. In the analysis performed in this thesis we utilise only the NH$_3$ (1,1) and (2,2) transitions so an explicit formula may be stated for the rotational temperature defined by these lines:

$$\frac{N_{2,2}}{N_{1,1}} = \frac{g_{2,2}}{g_{1,1}}\left(e^{-(E_{2,2}-E_{1,1})/kT_{rot}}\right).$$

Rearranging in terms of T_{rot} and inserting values for the constants we find

$$T_{rot} = -41\,K/\ln\left(\frac{3}{5}\frac{N_{2,2}}{N_{1,1}}\right), \tag{66}$$

where $g_{1,1} = 3$, $g_{2,2} = 5$ and $(E_{2,2} - E_{1,1})/k = 41\,K$. The column density in a particular state is proportional to $(\tau\,\Delta v)/A_{ul}$ via Equation 50, so Equation 66 may be written in terms of the optical depths of the NH$_3$ (1,1) and (2,2) lines:

$$T_{rot} = -41\,K/\ln\left(\frac{5}{3}\frac{A_{1,1}}{A_{2,2}}\frac{\tau_{2,2}}{\tau_{1,1}}\left[\frac{\Delta\nu_{2,2}}{\Delta\nu_{1,1}}\right]\right) = -41\,K/\ln\left(\frac{9}{20}\frac{\tau_{2,2}}{\tau_{1,1}}\left[\frac{\Delta\nu_{2,2}}{\Delta\nu_{1,1}}\right]\right), \tag{67}$$
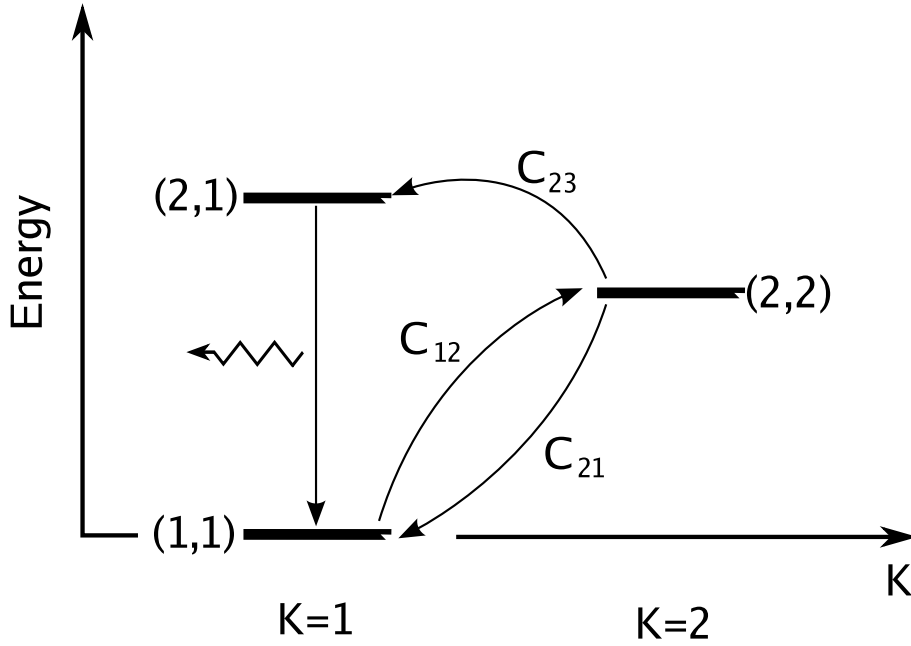
Figure 9: Energy level diagram showing the collisional transitions between the J,K=(2,2), (2,1) and (1,1) energy levels of NH$_3$. Quadrupole splitting is not shown. C$_{xy}$ are the collisional coefficients between levels. When calculating kinetic temperatures from the NH$_3$ (1,1) and (2,2) lines we must also take into account the non-metastable levels as they can still contain significant numbers of molecules. For temperatures under ~50 K it is sufficient to include only the J,K=(2,1) level.

Assuming the NH$_3$ (1,1) and (2,2) emission arises in the same gas then the linewidths should have the same value and $[\Delta\nu_{2,2}/\Delta\nu_{1,1}] \approx 1$. A comparison of the optical depths in the NH$_3$ (2,2) and (1,1) lines yields the rotation temperature from

$$\mathrm{T_{rot}} = -41\,\mathrm{K}/\ln\left(\frac{9}{20}\frac{\tau_{2,2}}{\tau_{1,1}}\right). \tag{68}$$

4: Calculate the kinetic temperature

In a simple two-level system in the steady state $\mathrm{n_u\,C_u = n_l\,C_l}$, (Equation 29), if radiative transitions are negligible. Assuming LTE conditions, and therefore a Boltzmann distribution of populations (Equation 18), and applying detailed-balance (Equation 30) we find that $\mathrm{T_{rot} = T_{kin}}$. However in the case of NH$_3$ the population in the non-metastable levels may be non-negligible. Hence the approximation of a Boltzmann distribution between the NH$_3$(1,1) and (2,2) levels may not be valid. If the excitation temperature is below ~50 K, we can improve our estimate of the kinetic temperature by considering collisions between the (1,1), (1,2) and (2,2) states (see Figure 9). The steady state equation for collisional transitions between these three states is

$$\frac{\mathrm{n_{22}}}{\mathrm{n_{11}}} = \frac{\mathrm{C_{12}}}{(\mathrm{C_{21} + C_{23}})} = \frac{\mathrm{C_{12}}}{\mathrm{C_{21}}}\frac{1}{(1 + \mathrm{C_{23}/C_{21}})}, \tag{69}$$

where C$_{23}$, C$_{21}$ and C$_{12}$ are the collisional rate coefficients between the J,K=(2,2→2,1), J,K=(2,2→1,1) and J,K=(1,1→2,2) levels, respectively. Substitution of the Boltzmann and detail balance relations for the factors $\mathrm{n_{22}/n_{11}}$ and $\mathrm{C_{12}/C_{21}}$ yields a new relationship between the rotational and kinetic temperatures:

$$\mathrm{T_{rot}} = \frac{\mathrm{T_{kin}}}{[1 + (\mathrm{T_{kin}}/41\,\mathrm{K})\ln(1 + \mathrm{C_{23}/C_{21}})]}. \tag{70}$$

Collisional rates have been modelled by Danby et al. (1988) and are given in Table 2.

Table 2: Collisional rates between the NH_3 (2,2), (1,1) and (2,1) rotational levels, from Danby et al. (1988).

Transition[a]	Collisional rates ($cm^3.s^{-1}$)			
	15 K	25 K	50 K	75 K
C_{23}	0.6×10^{-11}	1.0×10^{-11}	1.5×10^{-11}	1.7×10^{-11}
C_{21}	3.0×10^{-11}	2.8×10^{-11}	2.7×10^{-11}	2.8×10^{-11}
C_{23}/C_{21}	0.19	0.34	0.54	0.63

[a] $C_{23} = C(22 \rightarrow 21)$ is calculated from $C(21 \rightarrow 22)$ tabulated in Danby et al. (1988) via the detail balance equation ($C_{lu}/C_{ul} = e^{-(\Delta E)/T_{kin}}$), where ΔE is the energy difference between the energy levels ≈ 17.1 K.

5: Calculate the column density

Given the total integrated intensity ($\int_{-\infty}^{\infty} T_b\, dv$) in the NH_3 (1,1) spectrum, the column density in the J,K = 1,1 level may be found using Equation 52,

$$N_{1,1} = \frac{8k\pi\nu_{1,1}^2}{A_{ul}hc^3} \int_{-\infty}^{\infty} T_b\, dv \left(\frac{\tau}{1 - e^{-\tau}}\right),$$

where τ is the total optical depth in the NH_3 (1,1) spectrum. The total column density, N, may then be found from Equations 20 and 21, as before

$$N = \frac{N_{1,1}}{g_{1,1}} e^{(E_{1,1})/kT} Q(T_{rot}) \qquad\qquad Q(T_{rot}) = \sum_i g_i\, e^{-E_i/kT_{rot}},$$

where $Q(T_{rot})$ is the partition function. If only data for the (1,1) and (2,2) transitions are available then it is reasonable to approximate the partition function by a sum over the first few J,K energy levels. The total column density is then given by

$$N = N_{1,1} \left[\frac{1}{3} e^{+23.26/T_{rot}} + 1 + \frac{5}{3} e^{-41.18/T_{rot}} + \frac{14}{3} e^{-100.25/T_{rot}} + \frac{9}{3} e^{-177.21/T_{rot}} \right.$$

$$\left. + \frac{11}{3} e^{-272.02/T_{rot}} + \frac{26}{3} e^{-284.67/T_{rot}} \dots \right], \qquad (71)$$

which assumes that the relative population of all metastable levels of both ortho- and para-NH_3 are in thermal equilibrium at a temperature T_{rot}. Note that states with J = 3n have statistical weights of $2 \times (2J+1)$.

References

Danby G., Flower D. R., Valiron P., Schilke P., Walmsley C. M., 1988, MNRAS, 235, 229

Goldsmith P. F., Langer W. D., 1999, ApJ, 517, 209

Ho P. T. P., Martin R. N., Myers P. C., Barrett A. H., 1977, ApJ, 215, L29

Ho P. T. P., Townes C. H., 1983, ARA&A, 21, 239

Kukolich S. G., 1967, Physical Review, 156, 83

Loren R. B., Mundy L. G., 1984, ApJ, 286, 232

Oka T., Shimizu F. O., Shimizu T., Watson J. K. G., 1971, ApJ, 165, L15+

Rohlfs K., Wilson T. L., 2004, Tools of radio astronomy. Tools of radio astronomy, 4th rev. and enl. ed., by K. Rohlfs and T.L. Wilson. Berlin: Springer, 2004

Rydbeck O. E. H., Sume A., Hjalmarson A., Ellder J., Ronnang B. O., Kollberg E., 1977, ApJ, 215, L35

Townes C. H., Genzel R., Watson D. M., Storey J. W. V., 1983, ApJ, 269, L11

Townes C. H., Schawlow A. L., 1955, Microwave Spectroscopy. Microwave Spectroscopy, New York: McGraw-Hill, 1955

Ungerechts H., Walmsley C. M., Winnewisser G., 1980, A&A, 88, 259

Ungerechts H., Winnewisser G., Walmsley C. M., 1986, A&A, 157, 207